

Bioretention Cells Provide a 10-Fold Reduction in 6PPD-Quinone Mass Loadings to Receiving Waters: Evidence from a Field Experiment and Modeling

Timothy F. M. Rodgers,[†] Yanru Wang,[†] Cassandra Humes, Matthew Jeronimo, Cassandra Johannessen, Sylvie Spraakman, Amanda Giang, and Rachel C. Scholes*



Cite This: *Environ. Sci. Technol. Lett.* 2023, 10, 582–588



Read Online

ACCESS |

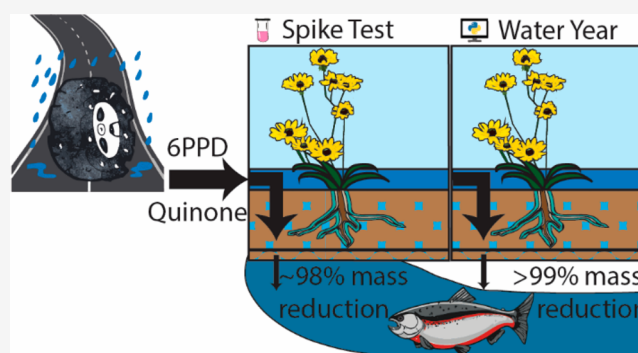
Metrics & More

Article Recommendations

Supporting Information

ABSTRACT: Road runoff to streams and rivers exposes aquatic organisms to complex mixtures of chemical contaminants. In particular, the tire-derived chemical 6PPD-quinone (*N*-(1,3-dimethylbutyl)-*N'*-phenyl-*p*-phenylenediamine-quinone) is acutely toxic to several species of salmonids, which are critical to fisheries, ecosystems, and Indigenous cultures. We therefore urgently require interventions that can reduce loadings of 6PPD-quinone to salmonid habitats. Herein, we conducted a spike and recovery experiment on a full-scale, mature bioretention cell to assess the efficacy of stormwater green infrastructure technologies in reducing 6PPD-quinone loadings to receiving waters. We then interpreted and extended the results of our experiment using an improved version of the “Bioretention Blues” contaminant transport and fate model. Overall, our results showed that stormwater bioretention systems can effectively mitigate >~90% of 6PPD-quinone loadings to streams under most “typical” storm conditions (i.e., < 2-year return period). We therefore recommend that stormwater managers and other environmental stewards redirect stormwater away from receiving waters and into engineered green infrastructure systems such as bioretention cells.

KEYWORDS: bioretention, stormwater, 6PPD-quinone, trace organic contaminants, fate models, green infrastructure, salmonids



INTRODUCTION

Road runoff to creeks, streams, and rivers exposes aquatic organisms to complex mixtures of chemical contaminants. Salmonids are anadromous or freshwater fish species that are frequently found in waters that receive road runoff. Wild or farmed salmonids are found in temperate waters around the globe and make up ~18% of global fisheries and aquaculture trade.¹ Salmonids are particularly important along the Pacific coast of North America, where they are keystone species of critical importance to many ecosystems² and Indigenous cultures.^{3,4}

This cultural, ecological, and economic importance means that in many areas managing threats to salmonid populations is important to maintaining socio-ecologically healthy aquatic environments. In streams in the U.S. Pacific Northwest, exposure to road runoff has been linked to the prespawning mortality of 40–90% of returning coho salmon (*Oncorhynchus kisutch*).⁵ For coho salmon, the primary toxicant in road runoff was recently discovered to be the compound 6PPD-quinone (*N*-(1,3-dimethylbutyl)-*N'*-phenyl-*p*-phenylenediamine-quinone), which is produced as a transformation product when atmospheric ozone reacts with 6PPD, an antiozonant tire

additive.⁶ 6PPD-quinone has been found at toxicologically relevant levels in many urban streams across North America,^{7–9} and in road dust in Japan,¹⁰ and further research has shown that a number of other salmonid species are impacted at environmentally relevant concentrations of 6PPD-quinone.^{11–13} 6PPD-quinone toxicity is an area of evolving research, with results indicating that juvenile salmon are also very sensitive to 6PPD-quinone exposure,¹⁴ that toxicity is not consistent among aquatic organisms, and that the modes of toxicity are not fully understood.¹⁵

We therefore urgently require interventions that can reduce loadings of 6PPD-quinone to salmonid habitats, particularly in urban areas along the Pacific coast of North America where sensitive populations and high loadings coincide. Regulators are currently assessing alternatives to 6PPD in car tires, but the

Received: March 17, 2023

Revised: May 26, 2023

Accepted: May 30, 2023

Published: June 16, 2023



development and adoption of alternatives, including the replacement of the current in-use stock of tires, will likely take many years.¹⁶ For instance, the California (USA) Department of Toxic Substances Control has proposed listing motor vehicle tires containing 6PPD as a “priority product”, which would require labeling and alternatives assessments by manufacturers, but would not ban its use. The Washington State (USA) Department of Ecology investigated alternatives to 6PPD, but concluded that it was difficult to determine if any alternative would be safer than 6PPD.¹⁷

Previous research suggests that bioretention systems or “rain gardens”,^{18,19} a type of “green infrastructure”, or “low impact development”^{20,21} technology, could be effective at reducing 6PPD-quinone loadings to urban streams. First, the physicochemical properties of 6PPD-quinone indicate that it could be partially captured by soil sorption.²² Further, in studies conducted before 6PPD-quinone was discovered as the primary causal toxicant in stormwater runoff, McIntyre et al.²³ and Spromberg et al.²⁴ found that stormwater filtered through laboratory-scale bioretention columns protected coho salmon from the acutely lethal effects of stormwater runoff. However, in a field-scale bioretention system preferential flow paths, differing loading patterns, and other factors can substantially impact bioretention system performance.^{25,26}

Herein, we conducted a 6PPD-quinone spike and recovery test on a full-scale bioretention cell in Vancouver, Canada. We interpreted and extended our analysis using the Bioretention Blues model of organic contaminant fate in bioretention systems.²² The goals of our study were to (A) Experimentally assess the effectiveness of mature bioretention systems for reducing the discharge of 6PPD-quinone, (B) model the performance of bioretention systems for removing 6PPD-quinone under different hydrological conditions, and (C) model dominant processes in 6PPD-quinone fate in bioretention systems and determine gaps in our understanding of those processes.

METHODS

Study Site. The studied bioretention system is located on the northeast corner of Pine and eighth Streets in Vancouver, Canada. It was constructed in summer 2021 and planted in fall 2021. The system area is 22 m², the contributing drainage area is 694 m², ponding depth is 15 cm, media depth is 45 cm with a layer of mulch on the surface, and the unlined bottom contains an underdrain wrapped in clear crush gravel and geotextile. Figures S1 and S2 show engineering drawings of the system, and SI section S1.1 gives additional site details.

Experimental Protocol. Our spike and recovery experiment was designed to represent the largest rainfall event that did not cause the system to overflow. We followed the experimental framework of Gu et al.²⁷ with some modifications. First, we conducted a “spike” test where chemicals (including 6PPD-quinone, bromide and rhodamine-WT) were added to the system while water was pumped from a water truck on July 28th, 2022. To assess whether 6PPD-quinone would be remobilized by rain events with small antecedent dry periods, we conducted a “flushing” test, where ~13m³ of water but no chemicals were added (Figure 1C) on August third, 2022. We took effluent samples from the system’s underdrain at a frequency of ~5–20 min for a total of 28 effluent and triplicate spike mixture samples during the spike test and 17 effluent samples during the flushing test. Further details are available in SI S1.2. Measured concentrations for 6PPD-

quinone, rhodamine-WT, and bromide, measured flow rates and other water quality parameters (temperature, pH, and conductivity), the version of the Bioretention Blues model used here, and all input model parametrization files (including an EPA-SWMM model of the catchment) can be found in our data repository²⁸ and from the cofirst author’s GitHub page.²⁹

Sample Extraction and Analysis. We quantified 6PPD-quinone by extracting the water samples using off-line solid-phase extraction (SPE), and analyzed 1 mL of well-mixed extract using an Agilent 1200 series high-performance liquid chromatography (HPLC) system and a 6410 triple quadrupole mass spectrometer (Agilent Technologies, CA, USA). Full details on the sample extraction and analysis are discussed in the SI (Section S1.3 and Table S1). We measured the concentrations of the bromide and rhodamine-WT tracers using ion chromatography (Dionex Aquion, Thermo Scientific, Ontario, Canada) and UV/vis spectroscopy (Unicam UV 300, Thermo Spectronic, USA), respectively.

Quality Assurance and Quality Control. We collected six field blanks, four background samples from the water truck, and two field duplicate samples. We created three additional duplicates by subsampling the volumes collected in the field. When analyzing our results, we replaced values below the MDL with half the MDL. We defined the method detection limit (MDL) as the mean field blank level plus either the 99 or the 98% confidence interval from the field blanks (Table S2).

Model Development, Parametrization, and Calibration. We developed an updated version of the Bioretention Blues²² model (Figure 1C) to help interpret the spike and recovery experiment and to extend our results to conditions and design configurations beyond those observed during the experiment (see SI S1.4 for full details).

We parametrized the updated Bioretention Blues model to represent the bioretention system at Pine and eighth St. in Vancouver, Canada. We calibrated the model hydrology using the Kling-Gupta efficiency (KGE)³⁰ between the measured and modeled outflows, and contaminant behavior using the conservative bromide and the sorptive rhodamine-WT tracers (full details in SI S1.4). We did not calibrate any parameters for 6PPD-quinone. We estimated the partition coefficients for 6PPD-quinone using BIOVIA COSMOtherm (version 21.0),^{31–34} the estimated values for log K_{OC} of 3.14 and the octanol–water partition coefficient (log K_{OW}) of 4.12 are both close to experimental values of 3.2–3.5, for log K_{OC} in road dust,¹⁰ and 4.3 for log K_{OW} .³⁵ We linearly interpolated the concentrations and flow rates between observations to generate a higher temporal resolution data set to use as inputs to the model (see additional parametrization details in SI S1.4).

Model Application. First, we modeled the spike and recovery experiment, using the fit between the measured and modeled values to evaluate the model, and the model outputs to help interpret the experimental results. Then, we used the model to extend our analysis and evaluate how a “typical” bioretention cell,¹⁸ represented by our system, would perform in reducing loadings of 6PPD-quinone to receiving bodies. We simulated single event time-series for 28 design storms across the intensity-duration-frequency (IDF) curves used by the City of Vancouver, and for a continuous simulation across a synthetic “average” water year used by the City of Vancouver that contains less intense events (see SI Section S1.5 for full details, Table S3 shows the rainfall intensities for the IDF

events and our data repository²⁸ contains the complete time-series used as inputs to the model).

We defined the “performance” of the system as its ability to reduce mass loadings and effluent concentrations of 6PPD-quinone. We assessed the “direct effluent” as the proportion of the influent mass that was released to the sewer network, through the underdrain or by overflowing. We defined the flow-weighted mean effluent concentration (MEC, ng L^{-1}) as the direct effluent mass of 6PPD-quinone divided by the total water volume entering the sewer network. We also calculated the acute risk quotient (RQ)³⁶ using the LC_{50} for adult coho salmon of 95 ng L^{-1} .⁹ We note that an LC_{50} of 41 ng L^{-1} was recently reported by Lo et al.¹⁴ for juvenile Coho salmon, using this value would increase all of the reported RQs by 2.3 times. We used the RQ to calculate an average (RQ_{av}) based on the MEC. An $\text{RQ}_{\text{av}} > 0.5$ indicates a “high” risk, $0.1 \leq \text{RQ}_{\text{av}} \leq 0.5$ the potential for acute risk, and $0.05 \leq \text{RQ}_{\text{av}} \leq 0.1$ the potential for acute risk to endangered species.³⁶

RESULTS AND DISCUSSION

Our results indicate that bioretention systems can effectively reduce 6PPD-quinone loadings in urban runoff. Despite the short hydraulic residence time (peak effluent concentrations were observed ~ 3 – 11 min after injection), our experimental results showed substantial mass and concentration reductions to the effluent for 6PPD-quinone. The observed flow rates (Figure 1a) indicated that water infiltrated rapidly into the studied system and then exfiltrated to the surrounding soil.

The bromide tracer (Figure 1b, orange) peaked within ~ 5 min and was flushed from the system in under an hour, exhibiting a right-skewed distribution. By contrast, the sorptive rhodamine-WT tracer peaked after ~ 3 min (Figure 1b, blue), but then had a long tail of continued detectable concentrations. This indicates that rhodamine-WT sorbed to the soil during the initial spike and then desorbed back into the flowing water. For 6PPD-quinone (Figure 1c), the experimental results indicated a mass reduction of $\sim 95\%$ to the underdrain. The peak effluent concentration of $\sim 150 \text{ ng L}^{-1}$ was substantially lower than the influent spike mixture concentration of $\sim 4300 \text{ ng L}^{-1}$, partially because the spike mixture was immediately diluted with injection water. Notably, there was a 7 min period where the concentration of 6PPD-quinone was above the LC_{50} of coho salmon (95 ng/L), but the concentration fell below the MDL (14 – 16 ng L^{-1}) within half an hour after spiking.

Model Evaluation and Results. The fit between measured and modeled data indicated that the Bioretention Blues model reproduced the processes involved in contaminant transport and fate in the bioretention cell during the spike and recovery experiment (Figure 1, see SI Section S2.1). The model showed adequate performance (defined as KGE values ≥ 0.5 , 1 indicates an ideal fit)^{22,37} for the calibrated flows (Figure 1a) and for the tracer compounds bromide and rhodamine-WT (Figure 1b). For 6PPD-quinone, the KGE modified to ignore bias in variances was 0.64 (Figure 1c, see SI Section S2.2).

Encouragingly, our results indicated that once captured 6PPD-quinone is unlikely to leach out of the bioretention system, at least over short interevent time scales. First, during our initial experiment we only saw detectable levels of 6PPD-quinone immediately following the spike injection. By contrast, concentrations of rhodamine-WT remained elevated throughout the experiment. This difference in fate was captured by our model, which predicted substantial remobilization of rhodamine-WT with the influx of clean water but predicted that 6PPD-quinone would mostly remain sorbed to the soil. Supporting this contention, during the flushing experiment, where we introduced $\sim 13 \text{ m}^3$ of clean water approximately 1 week after the initial spike experiment, we did not observe detectable effluent concentrations of 6PPD-quinone. For this event, the model predicted that $\sim 2\%$ of the influent mass would be remobilized to either the underdrain or to the surrounding soil. Although this lack of detection could have been caused by transformation or plant uptake of the 6PPD-quinone (given the uncertainty in the model parameters for those processes), it still showed that remobilization and leaching of 6PPD-quinone from fresh influent was not a substantial mass transport process, even given a very short interval (of < 1 week) between large events. Overall, across the modeled period the model estimated that $\sim 75\%$ of the influent 6PPD-quinone was retained by the soil, with $< 5\%$ released through the underdrain and $\sim 20\%$ exfiltrated to the surrounding soil (Figure 1d), with 2.5% predicted trans-

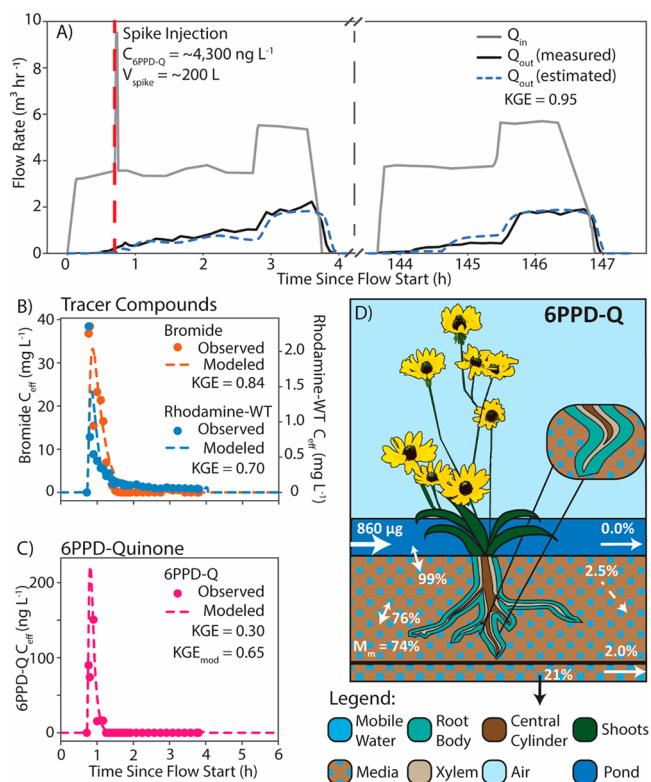


Figure 1. Overview of the results from the 6PPD-quinone (6PPD-Q) spike test. (A) Hydrology of the spike and recovery and flushing experiment, showing the measured influent and effluent flow rates, the modeled effluent flow rate (dashed line), and the timing of the spike injection. (B, C) Modeled (dashed lines) and measured (dots) effluent underdrain concentrations of the (B) calibrated tracer compounds and (C) uncalibrated 6PPD-quinone for the initial spike and recovery test period. (D) Modeled fate of 6PPD-quinone across the entire spike and flush test time period. Solid arrows represent mass transfers between compartments or into and out of the system, as a percentage of the influent mass (shown entering the ponding zone with units in μg); double-headed arrows indicate two-way processes with the larger arrowhead showing the dominant direction of exchange (e.g., 76% transfer from mobile water to media). Dashed lines represent primary transformation. M_m shows the percentage of influent mass retained by the soil.

amine-WT with the influx of clean water but predicted that 6PPD-quinone would mostly remain sorbed to the soil. Supporting this contention, during the flushing experiment, where we introduced $\sim 13 \text{ m}^3$ of clean water approximately 1 week after the initial spike experiment, we did not observe detectable effluent concentrations of 6PPD-quinone. For this event, the model predicted that $\sim 2\%$ of the influent mass would be remobilized to either the underdrain or to the surrounding soil. Although this lack of detection could have been caused by transformation or plant uptake of the 6PPD-quinone (given the uncertainty in the model parameters for those processes), it still showed that remobilization and leaching of 6PPD-quinone from fresh influent was not a substantial mass transport process, even given a very short interval (of < 1 week) between large events. Overall, across the modeled period the model estimated that $\sim 75\%$ of the influent 6PPD-quinone was retained by the soil, with $< 5\%$ released through the underdrain and $\sim 20\%$ exfiltrated to the surrounding soil (Figure 1d), with 2.5% predicted trans-

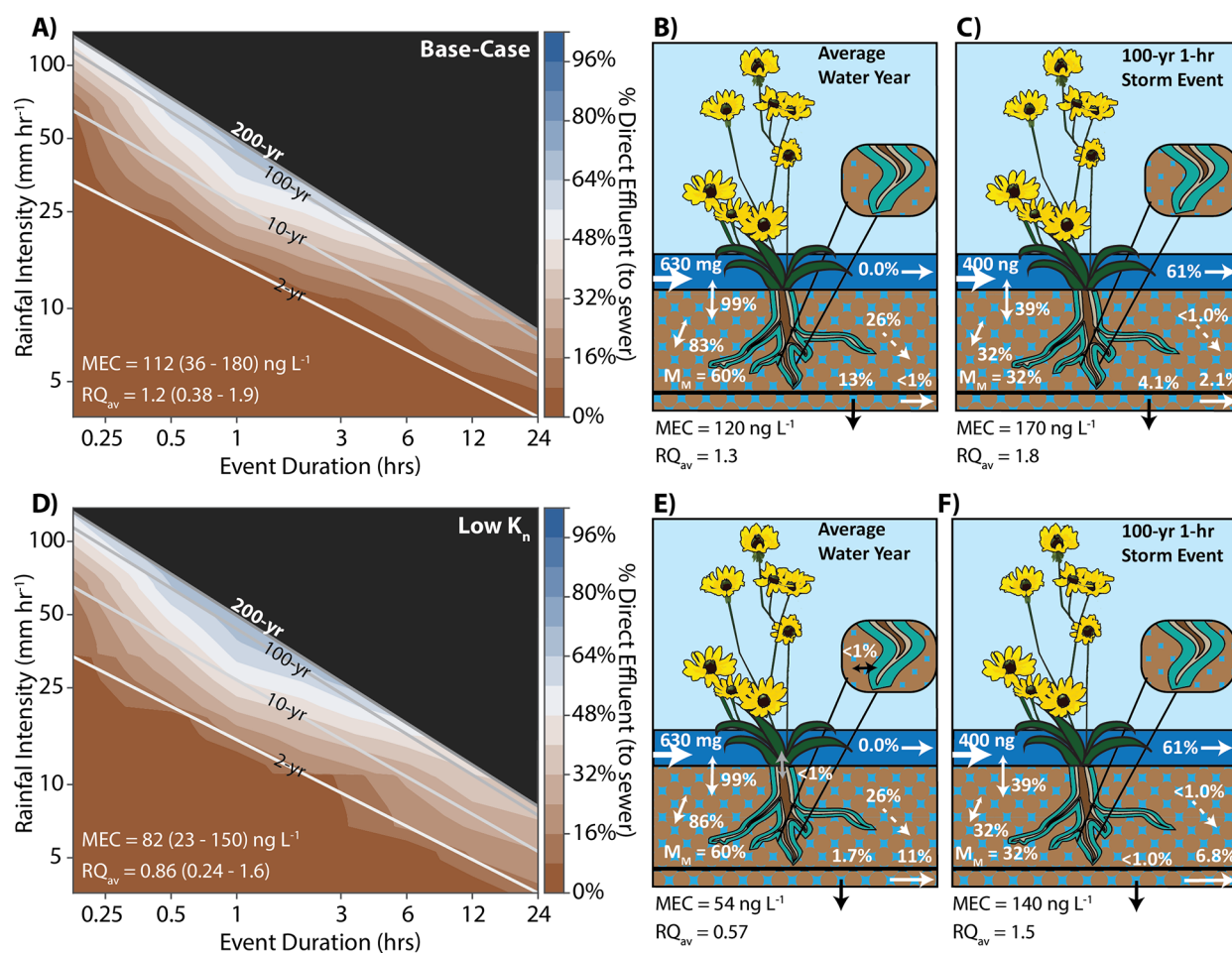


Figure 2. (A, D) Fate of 6PPD-quinone through the (A) studied and (D) low- K_n bioretention cell across the storm events defined by the City of Vancouver intensity-frequency-duration (IDF) curves. The contour colors (interpolated between the 28 simulated events) show the proportion of the influent mass that was advected through the bioretention cell to the sewer system, with brown colors representing less than 50% released and blue more than 50% released. The mean and range of the effluent concentrations (MEC) and the average risk quotients (RQ_{av}) are shown on the IDF figure. (B, E, C, F) Fate of 6PPD-quinone across (B, E) a synthetic “average” water year and (C, F) the City of Vancouver 100 year 1 h design storm event, respectively; E and F represent the low- K_n scenario. Solid arrows represent mass transfers between compartments or into and out of the system, as a percentage of the influent mass (shown entering the ponding zone with units in mg or ng); double-headed arrows indicate two-way processes with the larger arrowhead showing the dominant direction of exchange. Dashed lines represent primary transformation. M_m shows the percentage of influent mass retained by the soil.

formation in the soil compartment. SI Section S2.3 discusses limitations of our model and results.

Performance of Bioretention for 6PPD-Quinone. We ran the calibrated model for 28 events across the City of Vancouver intensity-duration-frequency (IDF) curves, assuming a constant 1000 ng L^{-1} influent concentration to represent a “worst-case” scenario, such as a system receiving effluent from a large highway (see SI section S1.5 for more details). Under these conditions, we predict that the as-built bioretention system would reduce mass-loadings of 6PPD-quinone to receiving systems by $>90\%$ for all events with a recurrence period of ≤ 2 years (Figure 2a). In an “average” water year, we predicted a reduction in annual mass loadings of $>95\%$, with 26% of the influent mass predicted to transform (Figure 2b), although we note that little is known about how quickly 6PPD-quinone is transformed in soil. Some uptake by plants may occur,³⁸ although this is likely minor in a fast-draining bioretention system such as this one.²² The system’s RQ_{av} ranged from 0.38 for the 2 year, 10 min event to 1.9 for the 200 year, 1 h event. For larger events, there were

substantial periods with an $RQ > 1$, indicating sustained effluent concentrations well above the LC_{50} for coho salmon.

The study system had a high exfiltration rate due to the high calibrated permeability ($\sim 125 \text{ mm h}^{-1}$) of the surrounding soil. To broaden the applicability of our results, we simulated the performance of a “low permeability” scenario consisting of an identical system situated in a soil with an infiltration rate of 3.3 mm h^{-1} , representing clayey or silty soils.³⁹ In this scenario, the system performed similarly to the as-built high permeability system, with more mass released to the sewer (e.g., 11% vs $<1\%$ for the studied system across the average water year), but a lower RQ_{av} of 0.24–1.6 across the 28 events due to the larger volume of underdrain flow diluting the effluent concentrations (Figure 2d). We note that since the Bioretention Blues model relies on system-specific calibrated parameters the uncertainty surrounding this simulated system is larger than for the as-built system.

For both the as-built and the low-permeability scenarios, this relatively high RQ_{av} (well above the US Environmental Protection Agency (EPA) threshold of >0.5 for a “high” risk) across all events was particularly driven by overflow of the

system during larger events (Figure 2c); water that overflowed the system received only minimal treatment due to settling and diffusion, leading to high combined effluent concentrations. On entering a stream, concentrations would be reduced through dilution. However, depending on the size of the stream, localized high concentrations would still be possible. Tire-derived chemicals such as 6PPD-quinone are believed to be rapidly mobilized by the first flush of a rainfall event,⁴⁰ meaning that the excellent performance for both the as-built and low permeability scenarios for smaller events and across an “average” water year could substantially reduce the risks to salmon. Larger events still present a risk, however, as in many catchments 6PPD-quinone is believed to exhibit an additional “middle flush”⁴⁰ of elevated concentrations of 6PPD-Q throughout the hydrograph.⁷ Design or management interventions could therefore improve the ability of bioretention systems to protect salmon from 6PPD-quinone during extreme events.

Environmental Implications. Overall, our results showed that mature, field-scale bioretention systems can effectively capture 6PPD-quinone in stormwater. Although finding safer alternatives to 6PPD will provide the most complete protection for salmonids and other potentially sensitive aquatic organisms, the efficacy of bioretention systems means that in the short term, stormwater managers can protect sensitive populations by redirecting runoff away from streams and toward engineered systems such as bioretention. Our modeling results indicate that under most “typical” storm conditions (e.g., <2 year return period) bioretention will greatly reduce the mass and concentration of 6PPD-quinone being directly released. Even during larger events, almost 50% of 6PPD-quinone may be captured, with the lower performance for the largest events driven mainly by overflow from the ponding zone. Although knowledge gaps remain regarding the transformation rates of 6PPD-quinone in soil, and the potential for transport through interflow and shallow groundwater flow, our results indicate that 6PPD-quinone is not likely to be remobilized from soil. Therefore, redirection to riparian zones or other vegetated areas may provide protection as well. By directing road runoff toward bioretention systems, stormwater managers and other environmental stewards can help protect salmonids and any other sensitive aquatic organisms from toxic road runoff and support socio-ecologically healthy aquatic environments.

■ ASSOCIATED CONTENT

Data Availability Statement

The data used in this paper, along with an archived version of the Bioretention Blues model code, is available from our data repository.²⁸ Current and future versions of the model are also available with an interactive tutorial from one of the lead authors' GitHub pages.²⁹

Supporting Information

The Supporting Information is available free of charge at <https://pubs.acs.org/doi/10.1021/acs.estlett.3c00203>.

Additional methodological details, including further information on the study site, experimental design, sample processing and analysis, and the model parametrization and calibration; additional results and discussion, including the calibrated model parameters, additional model evaluation details, and a discussion of limitations (PDF)

■ AUTHOR INFORMATION

Corresponding Author

Rachel C. Scholes – Department of Civil Engineering, University of British Columbia, Vancouver, British Columbia V6T 1Z4, Canada; orcid.org/0000-0001-5450-8377; Phone: 604-822-1987; Email: rachel.scholes@ubc.ca

Authors

Timothy F. M. Rodgers – Institute of Resources, Environment and Sustainability, University of British Columbia, Vancouver, British Columbia V6T 1Z4, Canada; orcid.org/0000-0003-1850-404X

Yanru Wang – Department of Civil Engineering, University of British Columbia, Vancouver, British Columbia V6T 1Z4, Canada

Cassandra Humes – Green Infrastructure Design Team, City of Vancouver Engineering Services, Vancouver V5Z 0B4, Canada

Matthew Jeronimo – School of Population and Public Health, University of British Columbia, Vancouver, British Columbia V6T 1Z9, Canada; orcid.org/0000-0001-8188-8993

Cassandra Johannessen – Department of Chemistry and Biochemistry, Concordia University, Montreal, Quebec H4B 1R6, Canada; orcid.org/0000-0001-8763-4994

Sylvie Spraakman – Green Infrastructure Design Team, City of Vancouver Engineering Services, Vancouver V5Z 0B4, Canada

Amanda Giang – Institute of Resources, Environment and Sustainability and Department of Mechanical Engineering, University of British Columbia, Vancouver, British Columbia V6T 1Z4, Canada; orcid.org/0000-0002-0146-7038

Complete contact information is available at:

<https://pubs.acs.org/10.1021/acs.estlett.3c00203>

Author Contributions

T.F.M.R.: Conception, investigation, data curation, methodology, software, writing (original draft), and visualization; Y.W.: Investigation, data curation, methodology, writing (original draft); C.H.: Investigation, methodology, writing (review and editing); M.J.: Investigation, methodology, writing (review and editing); C.J.: software (COSMOtherm), writing (review and editing); S.S.: Conception, investigation, data curation, methodology, writing (review and editing), supervision; A.G.: Conception, writing (review and editing), supervision; R.C.S.: Conception, investigation, methodology, writing (review and editing) and supervision.

Author Contributions

[†]T.F.M.R. and Y.W. contributed equally to this project.

Notes

The authors declare no competing financial interest.

■ ACKNOWLEDGMENTS

Many thanks to Sal Fuda and Colin Taylor for helping with sampling during the experiments; to Antonio Dias and Cayla Anderson for helping process samples for analysis; to Nick-Mead Fox for providing the SWMM model of the catchment and discussions around SWMM modeling; and to Prof. Elodie Passeport (University of Toronto) for helpful discussions regarding our experimental design. Computations were performed using infrastructure supported by CFI Innovation Fund to the Rapid Air Improvement Network (RAIN, grant number 39971). We would like to thank the Natural Sciences

and Engineering Research Council (NSERC) of Canada for an NSERC postdoctoral fellowship to T.F.M.R. and NSERC Discovery Grants to A.G. (RGPIN-2018-04893) and R.C.S. (RGPIN-2022-03115). We would also like to acknowledge that this research was conceptualized and implemented on the traditional, ancestral, and unceded territory of the Musqueam, Squamish, and Tsleil-Waututh peoples. As settler scholars, we are grateful to live, work, and learn as uninvited guests on these lands and we support the efforts of these communities, including their roles in stewarding, protecting, and restoring aquatic ecosystems.

REFERENCES

- (1) Food and Agriculture Organization of the United Nations (FAO). FISHSTAT, 2022. <https://www.fao.org/fishery/statistics-query/en/trade> (accessed 2023-01-19).
- (2) Walsh, J. C.; Pendray, J. E.; Godwin, S. C.; Artelle, K. A.; Kindsvater, H. K.; Field, R. D.; Harding, J. N.; Swain, N. R.; Reynolds, J. D. Relationships between Pacific Salmon and Aquatic and Terrestrial Ecosystems: Implications for Ecosystem-based Management. *Ecology* **2020**, *101* (9), e03060.
- (3) Carothers, C.; Black, J.; Langdon, S. J.; Donkersloot, R.; Ringer, D.; Coleman, J.; Gavenus, E. R.; Justin, W.; Williams, M.; Christiansen, F.; Samuelson, J.; Stevens, C.; Woods, B.; Clark, S. J.; Clay, P. M.; Mack, L.; Raymond-Yakoubian, J.; Sanders, A. A.; Stevens, B. L.; Whiting, A. Indigenous Peoples and Salmon Stewardship: A Critical Relationship. *E&S* **2021**, *26* (1), art16.
- (4) Campbell, S. K.; Butler, V. L. Archaeological Evidence for Resilience of Pacific Northwest Salmon Populations and the Socioecological System over the Last 7,500 Years. *E&S* **2010**, *15* (1), art17.
- (5) Scholz, N. L.; Myers, M. S.; McCarthy, S. G.; Labenia, J. S.; McIntyre, J. K.; Ylitalo, G. M.; Rhodes, L. D.; Laetz, C. A.; Stehr, C. M.; French, B. L.; McMillan, B.; Wilson, D.; Reed, L.; Lynch, K. D.; Damm, S.; Davis, J. W.; Collier, T. K. Recurrent Die-Offs of Adult Coho Salmon Returning to Spawn in Puget Sound Lowland Urban Streams. *PLoS One* **2011**, *6* (12), e28013.
- (6) Tian, Z.; Zhao, H.; Peter, K. T.; Gonzalez, M.; Wetzel, J.; Wu, C.; Hu, X.; Prat, J.; Mudrock, E.; Hettlinger, R.; Cortina, A. E.; Biswas, R. G.; Kock, F. V. C.; Soong, R.; Jenne, A.; Du, B.; Hou, F.; He, H.; Lundeen, R.; Gilbreath, A.; Sutton, R.; Scholz, N. L.; Davis, J. W.; Dodd, M. C.; Simpson, A.; McIntyre, J. K.; Kolodziej, E. P. A Ubiquitous Tire Rubber-Derived Chemical Induces Acute Mortality in Coho Salmon. *Science* **2021**, *371* (6525), 185–189.
- (7) Johannessen, C.; Helm, P.; Lashuk, B.; Yargeau, V.; Metcalfe, C. D. The Tire Wear Compounds 6PPD-Quinone and 1,3-Diphenylguanidine in an Urban Watershed. *Arch. Environ. Contam. Toxicol.* **2022**, *82*, 171–179.
- (8) Challis, J. K.; Popick, H.; Prajapati, S.; Harder, P.; Giesy, J. P.; McPhedran, K.; Brinkmann, M. Occurrences of Tire Rubber-Derived Contaminants in Cold-Climate Urban Runoff. *Environ. Sci. Technol. Lett.* **2021**, *8* (11), 961–967.
- (9) Tian, Z.; Gonzalez, M.; Rideout, C. A.; Zhao, H. N.; Hu, X.; Wetzel, J.; Mudrock, E.; James, C. A.; McIntyre, J. K.; Kolodziej, E. P. 6PPD-Quinone: Revised Toxicity Assessment and Quantification with a Commercial Standard. *Environ. Sci. Technol. Lett.* **2022**, *9* (2), 140–146.
- (10) Hiki, K.; Yamamoto, H. Concentration and Leachability of N-(1,3-Dimethylbutyl)-N'-Phenyl-p-Phenylenediamine (6PPD) and Its Quinone Transformation Product (6PPD-Q) in Road Dust Collected in Tokyo, Japan. *Environ. Pollut.* **2022**, *302*, 119082.
- (11) Hiki, K.; Yamamoto, H. The Tire-Derived Chemical 6PPD-Quinone Is Lethally Toxic to the White-Spotted Char *Salvelinus Leucomaenis Pluvius* but Not to Two Other Salmonid Species. *Environ. Sci. Technol. Lett.* **2022**, *9* (12), 1050–1055.
- (12) French, B. F.; Baldwin, D. H.; Cameron, J.; Prat, J.; King, K.; Davis, J. W.; McIntyre, J. K.; Scholz, N. L. Urban Roadway Runoff Is Lethal to Juvenile Coho, Steelhead, and Chinook Salmonids, But Not Congeneric Sockeye. *Environ. Sci. Technol. Lett.* **2022**, *9* (9), 733–738.
- (13) Brinkmann, M.; Montgomery, D.; Selinger, S.; Miller, J. G. P.; Stock, E.; Alcaraz, A. J.; Challis, J. K.; Weber, L.; Janz, D.; Hecker, M.; Wiseman, S. Acute Toxicity of the Tire Rubber-Derived Chemical 6PPD-Quinone to Four Fishes of Commercial, Cultural, and Ecological Importance. *Environ. Sci. Technol. Lett.* **2022**, *9*, 333.
- (14) Lo, B. P.; Marlatt, V. L.; Liao, X.; Reger, S.; Gallilee, C.; Brown, T. M. Acute Toxicity of 6PPD-quinone to Early Life Stage Juvenile Chinook (*Oncorhynchus Tshawytscha*) and Coho (*Oncorhynchus Kisutch*) Salmon. *Environ. Toxicol. Chem.* **2023**, *42* (4), 815–822.
- (15) Hiki, K.; Asahina, K.; Kato, K.; Yamagishi, T.; Omagari, R.; Iwasaki, Y.; Watanabe, H.; Yamamoto, H. Acute Toxicity of a Tire Rubber-Derived Chemical, 6PPD Quinone, to Freshwater Fish and Crustacean Species. *Environ. Sci. Technol. Lett.* **2021**, *8* (9), 779–784.
- (16) Dixon, S.; Goh, C.-Y. Tire-driven stormwater toxicity and salmon mortality from 6PPD-quinone. *Trends*, Aug 28, 2022. https://www.americanbar.org/groups/environment_energy_resources/publications/trends/2022-2023/september-october-2022/tire-driven-stormwater-toxicity/.
- (17) State of Washington Department of Ecology. Hazardous Waste and Toxics Reduction Program Technical Memo. https://www.ezview.wa.gov/Portals/_1962/Documents/6ppd/6PPD%20Alternatives%20Technical%20Memo.pdf.
- (18) Spraakman, S.; Rodgers, T. F. M.; Monri-Fung, H.; Nowicki, A.; Diamond, M. L.; Passeport, E.; Thuna, M.; Drake, J. A Need for Standardized Reporting: A Scoping Review of Bioretention Research 2000–2019. *Water (Switzerland)* **2020**, *12* (11), 3122.
- (19) Roy-Poirier, A.; Champagne, P.; Filion, Y. Review of Bioretention System Research and Design: Past, Present, and Future. *J. Environ. Eng.* **2010**, *136* (9), 878–889.
- (20) Ahiablame, L. M.; Engel, B. A.; Chaubey, I. Effectiveness of Low Impact Development Practices: Literature Review and Suggestions for Future Research. *Water, Air, and Soil Pollution* **2012**, *223* (7), 4253–4273.
- (21) Wang, J.; Banzhaf, E. Towards a Better Understanding of Green Infrastructure: A Critical Review. *Ecological Indicators* **2018**, *85*, 758–772.
- (22) Rodgers, T. F. M.; Wu, L.; Gu, X.; Spraakman, S.; Passeport, E.; Diamond, M. L. Stormwater Bioretention Cells Are Not an Effective Treatment for Persistent and Mobile Organic Compounds (PMOCs). *Environ. Sci. Technol.* **2022**, *56*, 6349.
- (23) McIntyre, J. K.; Davis, J. W.; Hinman, C.; Macneale, K. H.; Anulacion, B. F.; Scholz, N. L.; Stark, J. D. Soil Bioretention Protects Juvenile Salmon and Their Prey from the Toxic Impacts of Urban Stormwater Runoff. *Chemosphere* **2015**, *132*, 213–219.
- (24) Spromberg, J. A.; Baldwin, D. H.; Damm, S. E.; McIntyre, J. K.; Huff, M.; Sloan, C. A.; Anulacion, B. F.; Davis, J. W.; Scholz, N. L. Coho Salmon Spawner Mortality in Western US Urban Watersheds: Bioinfiltration Prevents Lethal Storm Water Impacts. *J. Appl. Ecol.* **2016**, *53* (2), 398–407.
- (25) de Macedo, M. B. de; do Lago, C. A. F. do; Mendiondo, E. M.; de Souza, V. C. B. Performance of Bioretention Experimental Devices: Contrasting Laboratory and Field Scales through Controlled Experiments. *RBRH* **2018**, *23*, DOI: 10.1590/2318-0331.0318170038.
- (26) Marvin, J. T.; Passeport, E.; Drake, J. State-of-the-Art Review of Phosphorus Sorption Amendments in Bioretention Media: A Systematic Literature Review. *Journal of Sustainable Water in the Built Environment* **2020**, *6* (1), DOI: 10.1061/JSWBAY.0000893.
- (27) Gu, X.; Rodgers, T. F. M.; Spraakman, S.; Van Seters, T.; Flick, R.; Diamond, M. L.; Drake, J.; Passeport, E. Trace Organic Contaminant Transfer and Transformation in Bioretention Cells: A Field Tracer Test with Benzotriazole. *Environ. Sci. Technol.* **2021**, *55* (18), 12281–12290.
- (28) Data for: Bioretention Cells Provide a Tenfold Reduction in 6PPD-Quinone Mass Loadings to Receiving Waters: Evidence from a Field Experiment and Modeling. *Hydroshare*, <https://doi.org/10.4211/hs.c24df560663448aebcbb9228c4fd4a19>.

- (29) Rodgers, T. F. M. Subsurface Sinks Model. *GitHub*, 2021. <https://github.com/tfmrodge/SubsurfaceSinks>.
- (30) Gupta, H. V.; Kling, H.; Yilmaz, K. K.; Martinez, G. F. Decomposition of the Mean Squared Error and NSE Performance Criteria: Implications for Improving Hydrological Modelling. *Journal of Hydrology* **2009**, *377* (1–2), 80–91.
- (31) Eckert, F.; Klamt, A. Fast Solvent Screening via Quantum Chemistry: COSMO-RS Approach. *AIChE J.* **2002**, *48* (2), 369–385.
- (32) Klamt, A. Conductor-like Screening Model for Real Solvents: A New Approach to the Quantitative Calculation of Solvation Phenomena. *J. Phys. Chem.* **1995**, *99* (7), 2224–2235.
- (33) Klamt, A.; Jonas, V.; Bürger, T.; Lohrenz, J. C. W. Refinement and Parametrization of COSMO-RS. *J. Phys. Chem. A* **1998**, *102* (26), 5074–5085.
- (34) *BIOVIA COSMOtherm Release*; Dassault Systèmes, 2023; <http://www.3ds.com>.
- (35) Walsh, J. C.; Pendray, J. E.; Godwin, S. C.; Artelle, K. A.; Kindsvater, H. K.; Field, R. D.; Harding, J. N.; Swain, N. R.; Reynolds, J. D. Relationships between Pacific Salmon and Aquatic and Terrestrial Ecosystems: Implications for Ecosystem-based Management. *Ecology* **2020**, *101* (9), e03060.
- (36) US EPA. *Technical Overview of Ecological Risk Assessment: Risk Characterization*; 2017. <https://www.epa.gov/pesticide-science-and-assessing-pesticide-risks/technical-overview-ecological-risk-assessment-risk> (accessed 2022-10-24).
- (37) Randelovic, A.; Zhang, K.; Jacimovic, N.; McCarthy, D.; Deletic, A. Stormwater Biofilter Treatment Model (MPiRe) for Selected Micro-Pollutants. *Water Res.* **2016**, *89*, 180–191.
- (38) Castan, S.; Sherman, A.; Peng, R.; Zumstein, M. T.; Wanek, W.; Hüffer, T.; Hofmann, T. Uptake, Metabolism, and Accumulation of Tire Wear Particle-Derived Compounds in Lettuce. *Environ. Sci. Technol.* **2023**, *57* (1), 168–178.
- (39) Hill, J. Low Permeability Soils. In *Low Impact Development Stormwater Management Planning and Design Guide*. Sustainable Technologies Evaluation Program, 2017; https://wiki.sustainabletechnologies.ca/index.php?title=Low_permeability_soils&mobileaction=toggle_view_desktop.
- (40) Peter, K. T.; Hou, F.; Tian, Z.; Wu, C.; Goehring, M.; Liu, F.; Kolodziej, E. P. More Than a First Flush: Urban Creek Storm Hydrographs Demonstrate Broad Contaminant Pollutographs. *Environ. Sci. Technol.* **2020**, *54* (10), 6152–6165.